sciendo

LATVIAN JOURNAL OF PHYSICS
AND TECHNICAL SCIENCES
2025, N 4

DOI: 10.2478/lpts-2025-0026

HETEREMOLECULAR STRUCTURE FORMATION IN BINARY SOLUTIONS OF DIMETHYLFORMAMIDE-WATER AND TETRAHYDROFURAN-WATER: FTIR AND REFRACTOMETRY

D. Bozorova[1,2]*, S. Gofurov[2], M. Ziyayev[3], A. Kokhkharov[1],
Z. Kadirova[2,4,5], O. Abdiraimova[4], O. Ismailova[1,2,6]

[1]Institute of Ion-Plasma and Laser Technologies,
33 Durmon Yuli Str., Tashkent, 100125, UZBEKISTAN
[2]Uzbekistan-Japan Innovation Center of Youth,
2B University Str., Tashkent 100195, UZBEKISTAN
[3]Namangan State University,
Namangan, 160107, UZBEKISTAN
[4]National University of Uzbekistan named after Mirzo Ulugbek,
4 University Str., Tashkent 100174, UZBEKISTAN
[5]Tashkent Institute of Chemical Technology,
32 Navoi Str., Tashkent, 100011, UZBEKISTAN
[6]Turin Polytechnic University in Tashkent,
17 Little Ring Road, Almazar district, Tashkent, 100195, UZBEKISTAN
*e-mail: bozorova191@gmail.com

Along with other works that employ a more complex and time-consuming approach to analyse the formation of heteromolecular structures in aqueous solutions of dimethylformamide and tetrahydrofuran, we propose a new technique based on the combined use of refractometry and IR spectroscopy. The formation of intermolecular complexes is analysed by measuring the excess refractive index and the ratio of OH absorption bands of bound molecules to those of free ones in the concentration range of 0÷1 mole fraction of components. It has been shown that the formation of heteromolecular structures occurs within a narrow concentration range of 0.3 to 0.4 mole fractions of dimethylformamide and tetrahydrofuran, which corresponds to the maximum number of realized hydrogen bonds in the dimethylformamide-water and tetrahydrofuran-water systems.

Keywords: *Excess refractive index, heteromolecular structures, infrared spectroscopy.*

1. INTRODUCTION

There are various experimental methods for investigating the properties of water and aqueous-organic solutions: dielectric [1], [2] and infrared spectroscopy [3]–[11], Raman spectroscopy [12]–[15], and terahertz spectroscopy [16]–[20], X-ray diffraction [21]–[23], neutron diffraction [24]–[28], proton magnetic resonance spectroscopy [29]–[31] and others. All these methods are highly sensitive to various structural and relaxation changes in molecules of liquids, allowing to establish specific mechanisms of their mutual dissolution in a wide range of component concentrations and solution temperatures and to register the formation of mono- and heteromolecular associates in solutions, as well as clathrate formations in aqueous mixtures almost any organic solvents.

Establishing a connection between the kinematic, dynamic, and spectral characteristics of molecules allows for a deeper understanding of the mechanism of intermolecular interactions in each particular case.

Understanding the processes of hydrogen bond formation plays a significant role in determining the structure and physicochemical properties of many structures and materials, and is intensively studied in physics, chemistry, biology, and interdisciplinary research. Systems with hydrogen bonds find use in various applied studies, for example, in crystal design [30], [31], [32], in the creation of systems with self-assembly [33], [34] and molecular recognition [35], [36], in hydrothermal synthesis [37], [38] and others.

For example, in [39], it was assumed from the similarity of the shapes of the OH group valence vibration lines in CCl4 solutions that such mixtures form complexes in an aprotic medium, but no direct evidence of the stoichiometry of the complexes was presented. Non-valent interactions in solution can also be studied by NMR [40]–[43] and vacuum ultraviolet spectroscopy [44]–[46]. In particular, the signals of protons involved in the formation of hydrogen bonds are usually shifted to a rather weak field. The difficulty of studying such systems like NMR spectroscopy lies in the rapid molecular and proton exchange, as a result of which chemical shifts are averaged over a set of all complexes and monomers coexisting in solution, as well as over an ensemble of possible hydrogen bonding geometries.

It should be noted that the choice of double aqueous-organic mixtures of water + dimethylformamide and water + tetrahydrofuran as the subject of research is due to their wide practical use in chemical synthesis [48]–[50], optical spectroscopy [51]–[54], EPR spectroscopy [55], [56], and high-performance liquid chromatography as mobile phases [57]–[60].

The refractometric parameters and their excess values make it possible to understand structural changes in binary and ternary solutions and provide valuable information about intermolecular interactions [61]–[63]. Thus, a review of the literature shows that there are no reports studying the combination of infrared spectroscopy and refractometry for aqueous solutions of dimethylformamide (DMF) and tetrahydrofuran (THF).

So far, in most studies, the information extracted from IR spectra has been obtained from the position of absorption bands, thus determining the main vibrational modes characteristic of individual molecules of mixtures. It was difficult to

interpret the absorption bands due to the overlap of nearby bands and the insufficient resolution of individual bands, associated with the need to increase the resolution in the IR spectra, which led to the impossibility of obtaining information on the formation of clusters, analysis of hydrogen bonds. Therefore, such information was obtained using other methods: dielectric permittivity [63]–[65], total isotropic Rayleigh scattering of coherent light [66]–[68], viscosity [69], [70], and excess molar mixing volume [71]–[74]. With the intensive development of modern interferometer devices, the time scale of spectrum recording has reduced dramatically from several minutes to seconds and the sensitivity of the method has increased significantly, allowing for obtaining information on intensities, half-widths, isotopic shifts, and other finer spectral parameters.

This work focuses on the investigation of structure formation through hydrogen bonding. For this purpose, the study of refractive indices, excess refractive indices, and IR spectra of aqueous solutions of DMF and THF was carried out at room temperature and atmosphere pressure over a wide range of concentrations.

2 EXPERIMENTAL

2.1 Materials

Standard grade tetrahydrofuran (C_4H_8O) (minimum assay 99.9 wt.%) and N,N-dimethylformamide (C_3H_7NO) (purity ~99.9 wt.%) obtained from Reagent Plus, as well as distilled water with pH=7.02 were used in the experiments. For preparation of aqueous solutions of THF and DMF, high-precision analytical scales EP 214C (Ohaus Explorer Pro, Switzerland) with an accuracy of ≤0.0002 g was used. Each aqueous-organic solution of a given composition was prepared separately and was not used in the preparation of solutions with different concentration of compositions.

2.2 Measurement

Refractive indices were measured using a high-sensitivity PAL-RI digital refractometer (ATAGO, Japan). The instrument measures refractive indices in the range of 1.3306–1.5284; the measurement error n is <0.0001.

Fourier transform infrared spectra were recorded on a Perkin Elmer Spectrum Two spectrophotometer with a signal-to-noise ratio of 9300:1 and a resolution of 0.5 cm^{-1} on a $LiTaO_3$ detector. The spectra of pure water, DMF, THF, and their mixtures were recorded in the wavelength range of 4000-400 cm^{-1}.

3 RESULTS AND DISCUSSION

3.1 Refractometric Properties

Precision measurements of the refractive indices (n^E) of a number of pure single-component liquids (water, DMF and THF), as well as aqueous solutions of DMF and

THF in a wide range of component concentrations were carried out at the wavelength of the D_2-line of the sodium atom (λ=589 nm) using a high-sensitivity refractometer. In order to avoid the possible influence of even minor temperature fluctuations both on the density of water and on the density of organic solvent, and therefore on the density of the aqueous organic solutions studied by us, all the experiments below were carried out in a closed thermostatically-controlled laminar flow box at a fixed temperature t=25±0.2 °C and atmospheric pressure.

The stability of the temperature in the measurement compartment was controlled by a built-in thermostat on a Peltier element. The duration of measuring the refractive index of each sample of the solution was no more than 5 seconds. 0.3 ml solution of each sample by three times was measured to ensure measurement accuracy and to avoid equipment error.

The excess refractive indices in terms of the refractive index of pure liquids and their binary solutions of molar composition x were calculated using the equation:

$$n^E = n_{mix} - (x_1 n_1 + x_2 n_2),$$

where x_1, x_2, n_1 and n_2, are the mole fractions and refractive indices of the first and second solvents in their solutions, respectively, and n_{mix} is the refractive index of the solution.

An important optical parameter that can exhibit ionic or molecular behaviour in a mixture is the refractive index, which is primarily determined by the structure of the molecule, wavelength, and temperature.

Table 1. Experimental Mole Fraction, Refractive Index, Excess Refractive Index and Excess Refractive Index for DMF-Water and THF-Water

x, DMF	*n*	n^E	*x,* THF	*n*	n^E
1.000	1.4272	0.0000	1.0000	1.4098	0.0000
0.897	1.4251	0.0077	0.9003	1.4088	0.0067
0.797	1.4239	0.0160	0.8025	1.4075	0.0130
0.702	1.4224	0.0235	0.6970	1.4051	0.0188
0.601	1.4200	0.0307	0.5977	1.4024	0.0237
0.498	1.4167	0.0371	0.4961	1.3990	0.0282
0.398	1.4113	0.0411	0.3972	1.3949	0.0320
0.302	1.4045	0.0435	0.2974	1.3860	0.0296
0.201	1.3904	0.0389	0.2002	1.3707	0.0228
0.099	1.3677	0.0259	0.1043	1.3574	0.0169
0.000	1.3324	0.0000	0.0000	1.3324	0.0000

The refractive index of the mixture depends on chemical rearrangements during mixing of solutions associated with electron polarizability, and the peak of the excess refractive index occurs when the physical properties of solvent-solvent processes change [64]. This can be shown from the calculated values of the excess refractive indices, where the n^E of the aprotic-protic solvent mixtures are higher than that of the protic-protic ones. In the THF-water and DMF-water systems, the refractive index values change monotonically with increasing molarity of aprotic liquids [64]. The refractive indices and calculated excess refractive indices of the THF-water and DMF-water mixtures are shown in Table 1. The refractive indices of the THF-water and DMF-water systems show a positive value along the x-axis (Fig. 1). We obtained deviations from the theoretical line, which indicates specific molecular interactions between various components.

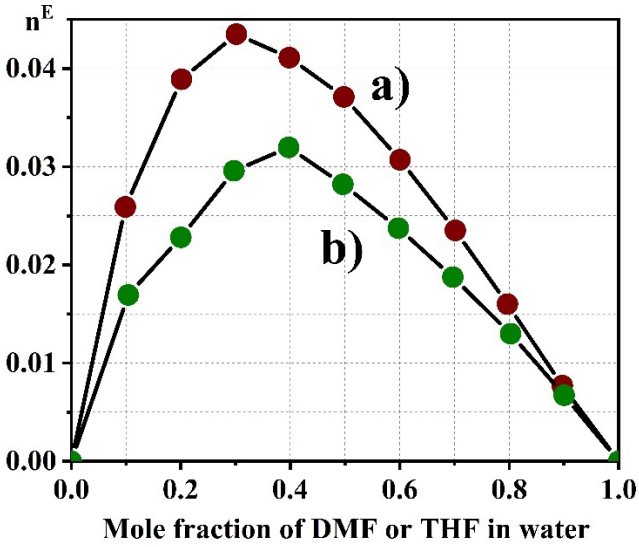

Fig. 1. Excess refractive index for binary solutions of DMF-water (a) and THF-water (b).

Figure 1 shows the excess refractive indices of DMF (a) and THF (b) in water, respectively, with different concentrations. The maximum of excess refractive indices corresponds to 0.3÷0.4 mole fraction of DMF and THF in the water. This is a good agreement with other literature data [63], [66], [68]. These maximum points represent the maximum number of interactions (intermolecular bonds) between DMF and water, as well as THF and water. These intermolecular bonds can be of different types, such as Van der Waals bonds, but they are more likely to be hydrogen bonds [13]. In comparing intermolecular interactions of water solutions, it is shown that the maximum value of the excess refractive indices of DMF-water is higher than that of THF-water. This result indicates that the solvent-solvent interaction of DMF-water is stronger in the same molar ratio of DMF and THF with water. Unlike the THF, the existence of nitrogen in the DMF makes both donor and acceptor bonds in the solution and strengthens bonds between DMF molecules and water [14], [15].

3.2 Infrared Spectra

Vibrational spectroscopy provides detailed and rare information about the intermolecular and intramolecular bonding interactions in liquids. Investigating vibrational frequency, changes in intensity and bandwidth offers valuable insight into the specific type of intermolecular interactions taking place in the liquid state. The infrared spectra of binary solutions of DMF-water and THF-water with a concentration range of 0–1 mole fraction were recorded. Figure 2 shows IR spectra of DMF-water (Fig. 2a) and THF-water (Fig. 2b) in the 3700–3000 cm^{-1} region.

The peak of maximum intensity in the spectra of DMF-water and THF-water is located at around 3400 cm^{-1}. Extremely wide spectra of OH stretching of both DMF-water and THF-water solutions undergo changes in integral intensity, as well as in

the contour shape and the ratio of intensities taken at low frequency to high-frequency field. The absorption band 3352 cm^{-1} of DMF-water shifts to 3500 cm^{-1}, absorption band of THF-water at 3352 cm^{-1} shifts to 3450 cm^{-1} as shown in Fig. 2b. These shifts in the OH stretching region indicate strong hydrogen bonding interactions between DMF and THF, respectively, with water molecules (Fig. 2a). At $X_{DMF} < 0.4$, hydrogen bonds between DMF and water molecules occur rapidly as a result of the disruption of the tetrahedral structure of water or the breaking of hydrogen bonds between water molecules. A similar phenomenon was observed in the DMF-water system by Raman spectroscopy [74]. Results of the exothermic enthalpies of DMF-water solution show at $x \approx 0.33$ mole fraction of DMF, the repulsive interaction between the hydrophobic groups (CH_3) and water drives the formation of larger, longer-lived molecular clusters. This repulsive interaction leads to energy being released, and the hydrogen bonds between DMF and water are stronger than hydrogen bonds between water molecules [74].

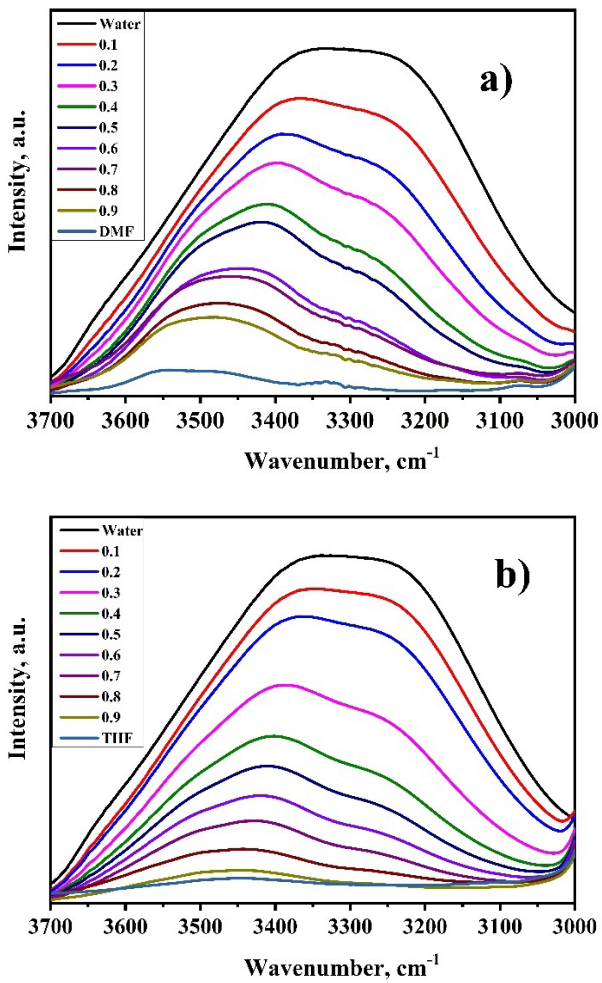

Fig. 2. Absorption bands 3000–3700cm^{-1} of OH-groups in the infrared spectra of DMF-water (a), and THF-water (b) solutions.

According to the measured IR spectra, it was shown that the mixture of water+THF forms complexes of 1:2 composition in the concentration range 0.1<x<0.4. It was shown that the hydration of THF occurred with the participation of weak hydrogen bonds $H_2O\cdots$H-C. It was also demonstrated that, in a narrow concentration range of 0.25–0.4 mole fraction of THF, the excess molar volume has a maximum characterising the formation of a dense structural packing of mixtures accompanied by strong interactions between molecules of both components [67], [69]. Excess molar volumes for the tetrahydrofuran + water system were calculated from experimentally measured densities and correlated using the Redlich-Kister equation [70]. The negative excess molar volume maxima also provide information about the presence of the following factors, such as strong specific interactions between hetero molecules via hydrogen bonds. The highest negative value of the molar volume is observed at a mole fraction of THF ~0.37 [67]. This indicates that the size of self-associated clusters formed by water molecules decreases with an increase in the molar fraction of THF in the concentration range and $0<X_{THF}<0.4$ [69]. The NMR data showed that the rotational motion of water molecules was most restricted at a concentration of $x \approx 0.3$ mole fraction of tetrahydrofuran, suggesting that the hydrogen bonds between water molecules were most immobile at this concentration.

The previous work [75] showed the ratio of absorption intensities at 3240 and 3360 cm^{-1} oscillation frequencies of OH-groups bound by strong and weak H-bonds for IR spectra of water-ethanol solutions. This ratio of absorption intensities by concentration of components allows obtaining information of stronger and quantity of H-bonds in solutions. In this work, we calculated the ratio of absorption intensities at 3246 cm^{-1} and 3352 cm^{-1} which corresponded to strong and weak hydrogen bonding, respectively (Fig. 3).

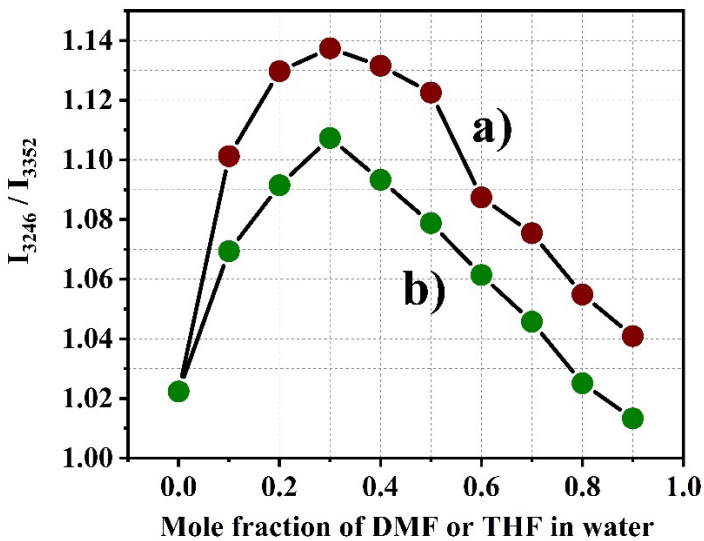

Fig. 3. Ratio of absorbance values taken at wavenumbers 3246 and 3360 cm^{-1} as a function of DMF (a) and THF (b) concentrations in solution.

DMF-water owns a wide maximum peak position, which includes 0.2–0.5 mole concentration of DMF in water, signified 0.3 mole DMF has strongest H-bonding, other concentrations like 0.2 and 0.4 closely make H-bonds in the solution. THF-water showed very sharp maximum of the peak at 0.3 mole fraction of THF in water, which formed 0.3 THF distinguishable strong H-bonds than other concentration. This result shows that hydrogen bond strengthening and significant structural rearrangement occur in the concentration range of $0.3<x<0.4$ mole fraction of DMF and THF. Both graphs show that the ratio passes through a maximum in the dissolved component concentration region of 0.3÷0.4 mole fraction. We interpret these results in terms of hydrogen bond saturation and maximum realization of the number of hydrogen bonds in mixtures within a narrow concentration range of DMF and THF. A comparative analysis of hydrogen bonding shows that water molecules are more strongly bonded to DMF than to THF. This IR analysis is in good agreement with the properties of H-bonds predicted by the refractive index excess. According to the purpose of the work, these two methods of analysis, complementing each other, are advantageous in obtaining quick and accurate information on H-bonds in the structure.

Another calculation for evaluating the characteristics of hydrogen bonds in mixtures was presented in the previous work [75]. Plotting deconvoluted the main symmetric and asymmetric OH stretching bands of Raman spectra, using Gaussian fitting characterised hydrogen bonds in DMF-water solutions [76]. As it is known, the spectral characteristics of hydrogen bonding represent three main spectral components with maxima of vibrations of strongly H-bonded OH-groups (3200 cm^{-1}), weakly H-bonded OH-groups (3400 cm^{-1}) and vibrations of free OH-groups (3650 cm^{-1}) [65]–[67], [73], [74].

To indicate changes in the infrared spectra, we calculated the ratio of optical density values which is the value of the speed of light passing through a sample. The corresponding Gaussian fitting results of pure water are shown in Fig. 2.

Detailed information of the Gaussian fitting to indicate symmetric and asymmetric H-bonding using IR spectrum of the pure water is given in Table 2. In the same way, we fitted all IR spectra DMF-water and THF-water solutions. Results of the detected peak position of symmetric and asymmetric H-bonds of pure water, as well as other mixtures are shown in Table 2.

Table 2. Peak Position of the Symmetric and Asymmetric H-Bonding of OH Group in DMF-Water and THF-Water Mixtures Detected by Gaussian Fitting of IR Spectra

Mole fraction of DMF	Asymmetric OH bonds (weak hydrogen bonds)	Symmetric OH bond (strong hydrogen bonds)
0	3183	3360
0.1	3201	3385
0.2	3241	3411
0.3	3250	3412
0.4	3257	3422
0.5	3258	3428
0.6	3279	3454
0.7	3277	3459
0.8	3282	3469
0.9	3292	3483

Mole fraction of THF	Asymmetric OH bonds (weak hydrogen bonds)	Symmetric OH bond (strong hydrogen bonds)
0	3183	3360
0.1	3227	3397
0.2	3229	3405
0.3	3225	3405
0.4	3246	3409
0.5	3258	3419
0.6	3241	3430
0.7	3268	3431
0.8	3272	3459
0.9	3270	3463

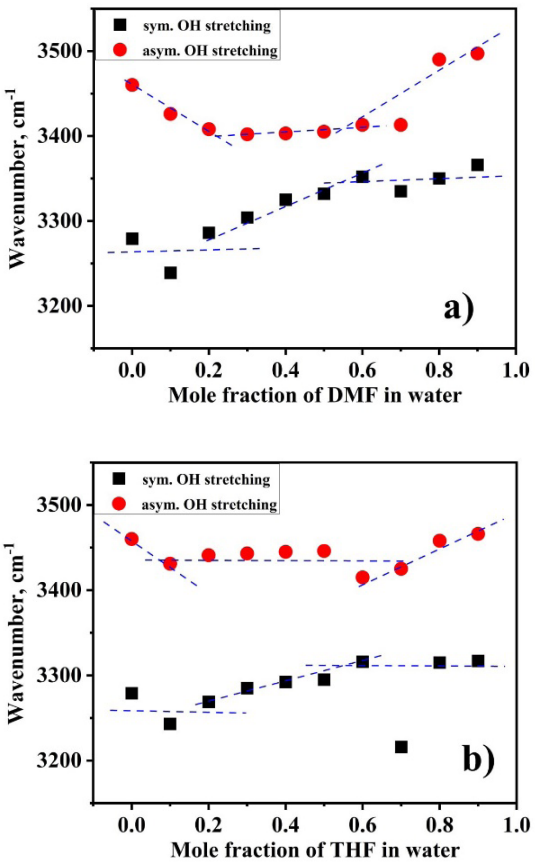

Fig. 4. Infrared intensity peaks of water with different mole fractions of DMF (a) and THF (b).

Figure 4 illustrates the infrared peak intensities of water at different X_{DMF} and X_{THF} in OH stretching vibration mode. Complexes are formed rapidly between water molecules and DMF and water molecules and THF molecules through the hydrogen bonds (Figs. 4a and 4b). At low concentration of DMF, the red shift of the

OH stretching vibration mode may be due to the fact that DMF barely weakens the tetrahedral structure of water [76]. However, very interestingly, at medium concentrations of DMF (0.3–0.5) a linear horizontal position is maintained, which we may consider as DMF replacing water molecules and DMF-water molecules creating a maximal number of hydrogen bonds and balancing with heterostructures of DMF-water and structures of water-water. Nevertheless, the OH stretching vibration mode quickly moves up at $X_{DMF} > 0.5$, which may be due to the fact that as the concentration of DMF increases in DMF-water mixtures, the tetrahedral structure of water is destroyed, resulting in the breaking of hydrogen bonds between water and water.

In the case of THF-water, we observed a clear boundary of changes at 0.3 mole of THF. Unlike the medium concentration effect of DMF on water molecules, THF enters into the water molecule network, which is formed due to hydrogen bonds, and linearly affects the structure of water by increasing its concentration. It can be seen that the critical point of the concentration of THF is 0.3, where the maximum H-bonds occur between molecules of THF and water. By increasing concentration of THF, hydrogen bonds weaken and decrease due to destroying water-water H-bonds, increasing THF-THF structures in the solutions.

4. CONCLUSIONS

By analysing the refractometry data in detail, it was found that structural changes occurred for DMF-water at ~0.3 mole fraction of DMF and THF-water at ~0.4 mole fraction of DMF. The studied two-component mixtures of THF-water and DMF-water belong to the category of solutions, in which not only intramolecular but also intermolecular complexes with H-bonding are formed, leading to compaction of solutions. The latter is confirmed by positive values of the excess refractive indices of all three binary mixtures in the entire range of component concentrations ($0<X<1$).

The established patterns of structural self-organization of binary solutions can be useful both for planning chromatographic experiments using two-component aqueous organic solvents as a mobile phase and for analysing the results obtained.

Thus, a novel approach based on the combined use of refractometry and IR spectroscopy is proposed to study structural changes in DMF-water and THF-water solutions over a concentration range from 0.0 to 1.0 mole fraction of components at room temperature and atmospheric pressure. It is shown that refractometry and IR spectroscopy are not only simple and accessible for studying aqueous solutions of aprotic solvents, but also extremely sensitive for detecting the formation of heteromolecular structures due to hydrogen bonds.

ACKNOWLEDGEMENTS

This study has been financially supported by the Foundation for Basic Research of the Academy of Sciences of Uzbekistan, the Ministry of Innovative Development of the Republic of Uzbekistan (grant No. FZ-202009029314) and Mirai Foundation.

REFERENCES

1. Esmonde-White, K., Lewis, M., & Lewis, I. R. (2022). Direct Measurement of Chocolate Components Using Dispersive Raman Spectroscopy at 1000 nm Excitation. *Applied Spectroscopy, 77* (3), 320–326.
2. Escoriza, M. F., Vanbriesen, J. M., Stewart, S., & Maier, J. (2006). Studying Bacterial Metabolic States Using Raman Spectroscopy. *Applied Spectroscopy, 60* (9), 971–976.
3. Xu, Y., Zhu, D., Song, Y., Zheng, X., & You, X. (2006). Hydrothermal Synthesis and Crystal Structure of the Novel Mixed Mo/V Meta-l-Oxygen Cluster Compound [Co(C2N2H8)(3)](4)[(Mo2Mo14V16O80)-Mo-V-V-VI-O-IV (PO4)(2)]Center Dot 10H(2)O Containing the Two Types of Typical Heteropoly Anions. The Journal of Molecular Structure, *782* (2), 165–170.
4. Sharma, A., Kaur, S., Mahajan C. G., Tripathi, S. K., & Saini, S. S. G. (2007). Fourier Transform Infrared Spectral Study of N, N′-Dimethylformamide-Water-Rhodamine 6G Mixture. Molecular Physics, 105 (1), 117–123.
5. Kanan, P. P., Arivazhagan, G., Sangeetha, T., Karthick, N. K., & Kumbharkhane A. C. (2021). FTIR Studies, DFT Calculations, and Time Domain Reflectometry Studies on TGF-Methanol Binary Solutions. Spectrochimica Acta, *Part A:* Molecular and Biomolecular Spectroscopy, 248, 119289.
6. Dwivedi, A., Baboo, V., & Bajpai. A. (2015). Fukui Function Analysis and Optical, Electronic, and Vibrational Properties of Tetrahydrofuran and Its Derivatives: A Complete Quantum Chemical Study. Journal of Theoretical Chemistry, 345234.
7. Ohashi, K., & Takeshita, H., (2021). Infrared Spectroscopic and Computational Studies of Co (ClO4)2 Dissolved in N, N-Dimethylformamide. Spectrochimica Acta, Part A: Molecular and Biomolecular Spectroscopy, 248, 119289.
8. Chalapathi, V. V., & Ramiah. K. V. (1966). Normal Vibrations of N, N-Dimethylformamide and N, N-Dimethylacetamide. *Proc. lnd. Acad. Sci, 64*, 148.
9. Tomar, D., Rana, B., & Jena. K. C. (2020). The Structure of Water–DMF Binary Mixtures Probed by Linear and Nonlinear Vibrational Spectroscopy. Journal of Chemical Physics, 152 (11), 114707.
10. Xu, Z., Li, H., Wang, C., Pan, H., & Han. S. (2006). The Methyl C–H Blueshift in N, N-Dimethylformamide-Water Mixtures Probed by Two-Dimensional Fourier-Transform Infrared Spectroscopy. Journal of Chemical Physics, 124 (24), 244502.
11. Biliškov, N., & Baranović, G. (2009). Infrared Spectroscopy of Liquid Water–N, N-Dimethylformamide Mixtures. The Journal of Molecular Liquids, 144 (3), 155–162.
12. Martínez-Reina, M., Amado-González, E., & Goméz-Jaramillo, W. (2015). Experimental Study and Modeling of the Refractive Indices in Binary and Ternary Mixtures of Water with Methanol, Ethanol and Propan-1-ol at 293.15 K. *Journal of* Solution Chemistry, *44* (2), 206–222.
13. Gofurov, Sh., Makhmanov, U., Kokhkharov, A., & Ismailova, O. B. (2019). Structural and Optical Characteristics of Aqueous Solutions of Acetic Acid. Applied Spectroscopy, 73 (5), 503–510.
14. Tomikawa, K., Kanno, H., & Kimoto, H. (2004). A Raman Study of Aqueous DMF and DMA Solutions at Low Temperatures. Canadian Journal of Chemistry, 82 (10), 1468–1473.
15. Pansare, K., Singh, S. R., Chakravarthy, V., Gupta, N., Hole, A., Gera, P., … & Krishna. C. M. (2020). EXPRESS: Raman Spectroscopy: An Exploratory Study to Identify Post-Radiation Cell Survival. *Applied Spectroscopy, 74* (5), 000370282090835.
16. Bozorova, D. T., Gofurov, Sh. P., Kokhkharov. A. M., & Ismailova O. B. (2021). Terahertz Spectroscopy of Aqueous Solutions of Acetic Acid. Journal of Applied Spectroscopy, 88 (4), 719–722.

17. Globus, T. R., Woolard, D. L., Khromova, T., Crowe, T. W., Bykhovskaia, M., Gelmont, B. L., … & Samuels, A.C. (2003). *THz-Spectroscopy of Biological Molecules.* Journal of Biological Physics, *29*, 89–100.
18. Ye, P., Meng, Q., Wang, G., Huang, H., Yang, Y., Su, B., & Zhang, C. (2022). Terahertz Spectroscopic Detection of Amino Acid Molecules under Magnetic Field. *Heliyon., 8* (11), 11414.
19. Wei, L., Yu, L., Jiaoqi, H., Guorong, H., Yang, Zh., & Weiling. F. (2018). Application of Terahertz Spectroscopy in Biomolecule Detection. *Frontiers in Laboratory Medicine, 2* (1), 127–133.
20. Lee. Y. S. (2009).*Terahertz Spectroscopy of Atoms and Molecules*. Principles of Terahertz Science and Technology. Springer, Boston, MA.
21. Mathlouthi, M. (1981). X-ray Diffraction Study of the Molecular Association in Aqueous Solutions of d-Fructose, d-Glucose, and Sucrose. *Carbohydrate Research, 91* (2), 113–123.
22. Kruh, R. F., & Standley, C. L. (1962). An X-Ray Diffraction Study of Aqueous Zinc Chloride Solutions. *Inorganic Chemisty, 1* (4), 941–943.
23. Adams, R., Balyuzi, H. H. M., & Burge, R. E. (1977). X-Ray Diffraction Studies of Aqueous Solutions of Urea. *J. Appl. Cryst., 10*, 256–261.
24. Gioacchino, M. Di., Bruni, F., & Ricci, M. A. (2019). N-Methylacetamide Aqueous Solutions: A Neutron Diffraction Study. *J. Phys. Chem. B. 123* (8), 1808–1814.
25. Kameda, Y., & Uemura, O. (1993). Neutron Diffraction Study on the Structure of Highly Concentrated Aqueous LiBr Solutions. *Bulletin of the Chemical Society of Japan, 66* (2), 384–389.
26. Ender, J. E. (1980). Neutron Diffraction, Isotopic Substitution and the Structure of Aqueous Solutions. Phil. Trans R. Soc. London. *B, Biological Sciences, 290*, 553–566.
27. Yamaguchi, T., Yoshida, K., Machida, Sh., & Hattori, T. (2022). Neutron Scattering on an Aqueous Sodium Chloride Solution in the Gigapascal Pressure Range. The Journal of Molecular Liquids, 365 (1), 120181.
28. Soper, A. K., Neilson, G. W., Enderby, J. E., & Howe, R. A. (1977). A Neutron Diffraction Study of Hydration Effects in Aqueous Solutions. Journal of Physics C: Solid State Physics, *10*, 1793.
29. Takahashi, H., Oue, T., & Sakai, M. (2020). Resonance IR Spectroscopy in Aqueous Solution by Combining IR Super-Resolution with TFD-IR Method. *Chemical Physics Letters, 758*, 137942.
30. Rabenstein, D. L., & Fan, S. (1986). Proton Nuclear Magnetic Resonance Spectroscopy of Aqueous Solutions: Complete Elimination of the Water Resonance by Spin-Spin Relaxation. *Analytical Chemistry, 58* (14), 3178–3184.
31. Martin, A., Nicholas, P., & Wasylishen, R. E. (1987). A Nuclear Magnetic Resonance Study of Aqueous Solutions of Several Nitrate Salts. *The Canadian Journal of Chemistry, 65* (5), 951–956.
32. Kokhkharov, A. M., Zakhidov, E. A., Gofurov, Sh. P., Bakhramov, S. A., & Makhmanov, U. K. (2013). Clusterization of Fullerene C70 Molecules in Solutions and Its Influence to Optical and Nonlinear Optical Properties of Solutions. *International Journal of Nanoscience, 12* (4), 1350027.
33. Patel, R. B., Stepanov, V., & Qiu, H. (2016). Dependence of Raman Spectral Intensity on Crystal Size in Organic Nano Energetics. *Applied Spectroscopy, 70* (8), 1339–1345.
34. Plastinin, I. V., Burikov, S. A., Gofurov, Sh. P., Ismailova, O. B., Mirgorod, Y., & Dolenko, T. A. (2020). Features of Self-Organization of Sodium Dodecyl-Sulfate in Water-Ethanol solutions: Theory and Vibrational Spectroscopy. *Journal of Molecular Liquids, 298*, 112053.
35. Cholli, A. L., & Lau, M. L. (1989). Simultaneous Detection of Optical Isomers and the Separation of Overlapping Resonances in a 1H NMR Spectrum of (+/-)-2,2-Dimethyl-1-Phenyl-1-Propanol Using an NMR Shift Reagent. *Applied Spectroscopy, 43* (7), 1168–1172.

36. Ismailova, O. B., Akhmedov, T. Kh., Igamberdiev, Kh. T., Mamatkulov, S. I., Saidov, A. A., Tursunov, S. O., & Khabibullaev, P.K. (2005). Heat-Capacity Anomaly in a Wide Vicinity of the Critical Point of the Triethylamine-Water Phase Transition. *Journal of Engineering Physics and Thermophysics, 78* (5), 1040–1045.
37. Larive, C. K., Jayawickrama, D., & Orfi, L. (1997). Quantitative Analysis of Peptides with NMR Spectroscopy. *Applied Spectroscopy, 51* (10), 1531–1536.
38. Flores-Castañeda, M., & Camacho-Lopez, S. (2023). Si Nanoparticle Decorated Bi2O2CO3 2D Nanocomposite Synthesized by Femtosecond Laser Ablation of Solids in Liquids and Aging. *Optics and Laser Technology, 158,* 108891.
39. Xu, Y., Zhu, D., Song, Y., Zheng, X., & You, X. (2006). Hydrothermal Synthesis and Crystal Structure of the Novel Mixed Mo/V Meta-l-Oxygen Cluster Compound [Co(C2N2H8)(3)](4)[(Mo2Mo14V16O80)-Mo-V-V-VI-O-IV (PO4)(2)]Center Dot 10H(2)O Containing the Two Types of Typical Heteropoly Anions. *The Journal of Molecular Structure, 782* (2), 165–170.
40. Mizuno, K. (2009). Roles of the Ether Oxygen in Hydration of TGF studied by IR, NMR and DFT Calculation Methods. *Journal of Physical Chemistry B, 113* (4), 906–915.
41. Weisenberger, L. A., & Koenig, J. L. (1989). NMR Imaging of Solvent Diffusion in Polymers. *Applied Spectroscopy, 43* (7), 1117–1126.
42. Davies, A. N., & Lampen, P. (1993). JCAMP-DX for NMR. *Applied Spectroscopy, 47* (8), 1093–1099.
43. Fischer, J. W., Merwin, L. H., & Nissan, R. A. (1995). NMR Investigation of the Thermolysis of Citric Acid. *Applied Spectroscopy, 49* (1), 120–126.
44. Larive, C. K., Jayawickrama, D., & Orfi, L. (1997) Quantitative Analysis of Peptides with NMR Spectroscopy. *Applied Spectroscopy, 51* (10), 1531–1536.
45. Shastri, A., Das, A. K., Krishnakumar, S., Singh, P. J., & Raja Sekhar, B. N. (2017). Spectroscopy of N, N-dimethylformamide in the VUV and IR Regions: Experimental and Computational Studies. *Journal of Chemical Physics, 147* (22), 224305.
46. Mao, J. X., Walsh, P., Kroll, P., & Schug, K. A. (2019). Simulation of Vacuum Ultraviolet Absorption Spectra: Paraffin, Isoparaffin, Olefin, Naphthene, and Aromatic Hydrocarbon Class Compounds. *Applied Spectroscopy, 74* (2), 72–80.
47. Cruse, C., Pu, J., & Goodpaster, J. V. (2020). EXPRESS: Identifying Thermal Decomposition Products of Nitrate Ester Explosives Using Gas Chromatography–Vacuum Ultraviolet Spectroscopy: An Experimental and Computational Study. *Applied Spectroscopy, 74* (12), 1486–1495.
48. Heravi, M. M., Ghavidel, M., & Mohammadkhan, L. (2018). Beyond a Solvent: Triple Roles of Dimethylformamide in Organic Chemistry. *RSC Adv., 8* (49), 27832–27862.
49. Muzart, J. (2009). N, N-Dimethylformamide: Much More than a Solvent. *Tetrahedron, 65* (40), 8313–8323.
50. Zhu, Y., Yang, J., Mei, F., Li, X., & Zhao, Ch. 2022). Bio-Based 1,4-Butanediol and Tetrahydrofuran Synthesis: Perspective. *Green Chemistry, 24*, 6450–6466.
51. Angle, S. R., & El-Said, N. A. (2002). Stereoselective Synthesis of Tetrahydrofurans via Formal [3+2]-Cycloaddition of Aldehydes and Allylsilanes. Formal Total Synthesis of the Muscarine Alkaloids (−)-Allomuscarine and (+)-Epimuscarin. *Journal of the American Chemical Society, 124* (14), 3608–3613.
52. Sałdyka, M., Mielke, Z., & Haupa, K. (2018). Structural and Spectroscopic Characterization of DMF Complexes with Nitrogen, Carbon Dioxide, Ammonia and Water. Infrared Matrix Isolation and Theoretical Studies. *Spectrochimica Acta - Part A: Molecular and Biomolecular Spectroscopy, 190*, 423–432.
53. Shastri, A., Das, A. K., Krishnakum, S., Singh, P. J., & Sekhar, B. N. R. (2017). Spectroscopy of N, N-Dimethylformamide in the VUV and IR Regions: Experimental and Computational Studies. The Journal of Chemical Physics, 147, 224305.

54. Liu, B., & Bazan, G. C. (2007). Tetrahydrofuran Activates Fluorescence Resonant Energy Transfer from a Cationic Conjugated Polyelectrolyte to Fluorescein-Labeled DNA in Aqueous Media. *Chemistry: An Asian Journal, 2* (4), 499–504.
55. Nawrocki, P. R., & Sørensen, T. J. (2023). Optical Spectroscopy as a Tool for Studying the Solution Chemistry of Neodymium (iii). *Physical Chemistry Chemical Physics, 25*, 19300–19336.
56. Reszka, K., Kolodziejczyk, P., & Lown, J. W. (1988). Photosensitization by Antitumor Agents. 5. Daunorubicin-Photosensitized Oxidation of NAD (P)H in Aqueous and N, N-Dimethylformamide/Aqueous Solutions – An Electron Paramagnetic Resonance Study. *Free Radical Biology and Medicine, 5* (2), 63–70.
57. Hunold, J., Eisermann, J., Brehm, M., & Hinderberger, D. (2020). Characterization of Aqueous Lower-Polarity Solvation Shells Around Amphiphilic 2,2,6,6-Tetramethylpiperidine-1-oxyl Radicals in Water. *Journal of Physical Chemistry B, 124* (39), 8601–8609.
58. Dembek, M., & Bocian, S. (2020). Pure Water as a Mobile Phase in Liquid Chromatography Techniques. *Trends in Analytical Chemistry, 123*, 115793.
59. Clifford, M. J., & Eastwood, D. (2004). Design of a Novel Passive Solar Tracker. *Solar Energy, 77* (3), 269–280.
60. Sanganal, S. K., Kulkarni, G. B., & Karegoudar, T. B. (2013). Development and Validation of High Perfomance Liquid Chromatographic Analysis of Residual N, N-Dimethylformamide in Spent Medium after Biodegradation by Paracoccus denitrificans SD1. *ISRN Chromatography 2013*, 1–6.
61. Góra, R., Hutta, M., & Rohárik, P. (2012). Characterization and Analysis of Soil Humic Acids by Off-Line Combination of Wide-Pore Octadecylsilica Column Reverse Phase High Performance Liquid Chromatography with Narrow Bore Column Size-Exclusion Chromatography and Fluorescence Detection. *Journal of Chromatography A, 1220*, 44–49.
62. Aliaj, F., Bytyqi-Damoni, A., & Syla, N. (2016). Density and Refractive Index Study of the Ternary System Benzene-Ethanol-Hexane. *AIP Conference Proceedings, 1722*, 290015.
63. Moosavi, M., & Rostami, A. A. (2016). Densities, Viscosities, Refractive Indices, and Excess Properties of Aqueous 1,2-Etanediol, 1,3-Propanediol, 1,4-Butanediol, and 1,5-Pentanediol Binary Mixtures. *Journal of Chemical & Engineering Data, 62* (1), 156–168.
64. El-Dossoki, F. I. (2007). Refractive Index and Density Measurements for Selected Binary Protic-Protic, Aprotic-Aprotic, and Aprotic-Protic Systems at Temperatures from 298.15 K to 308.15 K. *JCCS, 54* (5), 1129–1137.
65. Mohammadi, L., & Omrani, A. (2017). Density, Refractive Index, and Excess Properties of Sulfolane and Alkanediols Binary Mixtures at Different Temperatures. *Journal of Thermal Analysis and Calorimetry, 131* (3).
66. Komudzińska, M., Tyczyńska, M., Jóźwiak, M., Burakowski, A., & Gliński, J. (2020). Volumetric, Acoustic and Thermal Properties of Aqueous N, N-Dimethylformamide System. Effect of Temperature and Composition. *Journal of Molecular Liquids, 300*, 112321.
67. Nayak, J. N., Aralaguppi, M. I., Kumar Naidu, B. V., & Aminabhavi, T. M. (2004). Thermodynamic Properties of Water + Tetrahydrofuran and Water + 1,4-Dioxane Mixtures at (303.15, 313.15, and 323.15) K. *Journal of Chemical & Engineering Data, 49* (3), 468–474.
68. Razzokov, D., Ismailova, O. B., Mamatkulov, Sh. I., Trunilina, O. V., & Kokhkharov, A. M. (2014). Heteromolecular Structures in Aqueous Solutions of Dimethylformamide and Tetrahydrofuran, According to Molecular Dynamics Data. *Russian Journal of Physical Chemistry A, 88*, 1500–1506.
69. Katayama, M., & Ozutsumi, K. (2008). The Number of Water-Water Hydrogen Bonds in Water-Tetrahydrofuran and Water-Acetone Binary Mixtures Determined by Means of X-Ray Scattering. *Journal of Solution Chemistry, 37* (6), 841–856.

70. Jones, G., & Talley, S. K. (1933). The Viscosity of Aqueous Solutions as a Function of the Concentration. *Journal of the American Chemical Society, 55* (2), 624–642.
71. Sharma, A., Kaur, S., Mahajan, C. G., Tripathi, S. K., & Saini, S. S. G. (2007). Fourier Transform Infrared Spectral Study of N, N′-Dimethylformamide-Water-Rhodamine 6G Mixture. *Molecular Physics, 105* (1), 117–123.
72. Tomikawa, K., Kanno, H., & Kimoto, H. (2004). A Raman Study of Aqueous DMF and DMA Solutions at Low Temperatures. *Canadian Journal of Chemistry, 82* (10), 1468–1473.
73. Gogolinskaya, T. A., Patsaeva, S. V., & Fadeev, V. V. (1986). On the Regularities of Change of the 3100–3700 см$^{-1}$ Band of Water Raman Scattering in Salt Aqueous Solutions. *Doklady Akademii Nauk, 290* (5), 1099–1103.
74. Cilense, M., Benedetti, A. V., & Vollet, D. R. (1983). Thermodynamic Properties of Liquid Mixtures. II. Dimethylformamide-Water. *Thermochima Acta, 63* (2), 151–156.
75. Burikov, S., Dolenko, T., Patsaeva, S., Starokurov, Y., & Yuzhakov, V. (2010). Raman and IR Spectroscopy Research on Hydrogen Bonding in Water-Ethanol Systems. *Molecular Physics, 108* (18), 2427–2436.
76. Yang, B., Lang, H., Liu, Z., Wang, S., Men, Z., & Sun, C. (2021). Three Stages of Hydrogen Bonding Network in DMF-Water Binary Solution. *Journal of Molecular Liquids, 324*, 114996.